

Superelasticity and Impact Properties of Two Shape Memory Alloys: $\text{Ti}_{50}\text{Ni}_{50}$ and $\text{Ti}_{50}\text{Ni}_{48}\text{Fe}_2$

J.-C. Brachet, P. Olier*, G. Brun, P. Wident, I. Tournie, C. Foucher and P. Dubuisson

CEA/CEREM/SRMA, CEA Saclay, 91191 Gif-sur-Yvette, France

* CEA/CEREM/CE2M, CEA Saclay, 91191 Gif-sur-Yvette, France

Abstract. Superelasticity phenomena and Impact behaviour have been studied on $\text{Ti}_{50}\text{Ni}_{50}$ and $\text{Ti}_{50}\text{Ni}_{48}\text{Fe}_2$ shape memory alloys. Both alloys have been made by powder metallurgy (combustion synthesis). The main objective of the present work was to induce superelastic properties for temperatures ranging from -25°C to 0°C on a TiNi-based alloy by the addition of 2% Fe. It is well known that superelasticity properties are enhanced by the occurrence of premartensitic R phase transition. On the other hand, Fe addition decreases the martensitic transformation temperature (M_s) promoting the occurrence of intermediate "premartensitic" R phase. For binary TiNi alloys, cold working and partial recovery heat treatment is necessary to obtain such as properties.

This paper describes the microstructure, superelasticity and Charpy Impact behaviour of both $\text{Ti}_{50}\text{Ni}_{50}$ and $\text{Ti}_{50}\text{Ni}_{48}\text{Fe}_2$. Results have shown that :

Impact energy curves display unexpected trend for testing temperatures ranging from -196 to $+50^\circ\text{C}$. In particular, for TiNiFe alloy, typical Impact energy values are : $25\text{J}/\text{cm}^2$ at -196°C , $4\text{J}/\text{cm}^2$ at -25°C (the minimal value obtained) and $20\text{J}/\text{cm}^2$ at $+20^\circ\text{C}$. Complementary fractographic examinations have shown a brittle fracture mode for test temperatures ranging from -25 to 0°C . On the other hand, these temperatures correspond to the maximum of superelasticity, that is 1.5 to 2% of reversible strain measured by loading and unloading during tensile test. These results show a high brittleness probably induced by the intermediate "R" phase. Consequently, the optimization of superelasticity should be detrimental to the ductility/toughness of the TiNi alloys.

1. INTRODUCTION

TiNi based materials are the main Shape Memory Alloys (SMA) used for industrial applications due to their attractive thermomechanical properties. Especially, the superelastic properties of this type of SMA have been used for different type of applications. So, it is of technological importance to get a better understanding of the mechanical behaviour of TiNi based alloy showing superelasticity.

The present work is devoted to get some insight of the ductility/toughness characteristics of TiNi-SMA in the specific temperature range corresponding to the superelastic behaviour. Two alloys have been studied: the first one is an equiatomic TiNi alloy which is considered as a reference, the second one is a $\text{Ti}_{50}\text{Ni}_{48}\text{Fe}_2$. It has been already observed that by substituting Fe for Ni in TiNi, one can decrease the M_s temperature more strongly than the "premartensitic" R phase start temperature (R_s) [1] [2] [3] [4]. On the other hand, it has been shown that by using cold-working and subsequent annealing in the range 350 - 500°C , one can obtain the same evolution (i.e. important decrease of M_s and occurrence of R phase intermediate transformation) on binary TiNi SMA [5] [6] [7]. Moreover, it seems that the occurrence of intermediate R phase transformation in TiNi SMA enhances superelastic properties [8]. So, in the present study, the addition of 2%Fe on a TiNi alloy has been made to promote superelastic properties in a lower temperature range ($<0^\circ\text{C}$) than it is possible for a near equiatomic TiNi-SMA, by the occurrence of R phase transformation without the need of cold-working and subsequent annealing. Another objective of the present work was to characterize the Charpy impact properties of the alloys. For this last point, very few data are available in the literature [9].

2. MATERIAL

The both alloys have been produced by powder metallurgy, through an original combustion synthesis procedure [10]. Then, the ingots were hot extruded and homogenized at 900°C. The equiatomic TiNi alloy was cold-rolled (10%) and annealed 20min. at 450°C to promote the occurrence of intermediate R phase transformation and so, to enhance superelastic properties as already discussed. The $Ti_{50}Ni_{48}Fe_2$ alloy was just homogenized after hot extrusion. The chemical content of each alloy is shown on table 1.

Table 1 / Chemical content (at.%) of the alloys studied.

	Ti	Ni	Fe	C	O	N
$Ti_{50}Ni_{50}$	49.83	49.73	0.028	0.102	0.303	0.0087
$Ti_{50}Ni_{48}Fe_2$	49.77	47.65	2.16	0.15	0.26	0.0091

3. RESULTS AND DISCUSSION

3.1 Phase transformation temperatures

Typical phase transformation temperatures measured by Dilatometry and Differential Scanning Calorimetry (DSC) for the homogenized metallurgical state are presented in table 2.

Table 2 / Typical phase transformation temperatures (°C) of the alloys after homogenization at 900°C, measured by dilatometry (heating/cooling rate = 1°C/s) and by DSC (heating/cooling rate = 5°C/min.).

	Table 2-a : $Ti_{50}Ni_{50}$ Alloy			
	On cooling : Aust. => Mart.		On heating : Mart. => Aust.	
	Ms	Mf	As	Af
Dilatometry	21	-4	30	45
DSC	10	-15(+/-5)	25	45(+/-5)

	Table 2-b : $Ti_{50}Ni_{48}Fe_2$ Alloy							
	On cooling : Aust. => R Phase => Mart.				On heating : Mart. => R Phase => Aust.			
	Rs	Rf	Ms	Mf	Rs	Rf	As	Af
Dilatometry	-16	-33	-104	< -120	-72	-53	-27	-14
DSC	-10	-28	-110	< -120	-60 (*)		-20 (*)	

(*) For $Ti_{50}Ni_{48}Fe_2$ alloy, DSC results on heating do not allow to deconvolute the both stages of phase transformation (that is : Martensite => R Phase and then R Phase => Austenite)

From table 2 one can notice that dilatometry and DSC give coherent results. Equiatomic $Ti_{50}Ni_{50}$ alloy display quite low values of transformation temperatures (Ms = 10-20°C). One can correlate this trend to the nominal content of oxygen in the alloy [11]. For $Ti_{50}Ni_{48}Fe_2$ alloy, Fe addition has contributed to decrease strongly the Ms temperature and to promote the occurrence of intermediate R phase transformation for temperatures ranging from -35°C up to -15°C. On the other hand, one can remark that the {R phase \Leftrightarrow Austenite} transformation display a very small hysteresis between cooling and heating (< 6°C). This last point is of interest to obtain optimized superelastic properties.

3.2 Microstructure

Optical observations (fig. 1) after electrolytic polishing show an important precipitation lying along the hot extrusion direction. This precipitation is mainly constituted of Ti_4Ni_2O type oxides [10] [11], as confirmed by analytical Transmission Electron Microscopy (TEM) examinations. The grain size can be

evaluated by using polarized light [12] (fig. 2). The optical micrographs of figure 2 show that the grain size is quite heterogeneous with typical sizes ranging from 10 to 100 μm and with a textured morphogology (as for precipitates, the grains are elongated in the hot extrusion direction).

Some complementary TEM examinations on thin foils have been made. Typical electron micrographs are shown on figure 3. These micrographs show that for $\text{Ti}_{50}\text{Ni}_{50}$ alloy, the matrix structure is biphased (that is : equiaxed grains of austenite and very fine laths of martensite) and that for $\text{Ti}_{50}\text{Ni}_{48}\text{Fe}_2$ alloy, the matrix is pure austenite. On the other hand, TEM examinations have allowed to verify the cristallographic structure of precipitates which is consistent with a $\text{Ti}_4\text{Ni}_2\text{O}$ type oxide [11].

3.3 Superelastic and Charpy impact properties.

The superelastic properties have been estimated by specific tensile test using extensometry (to allow accurate measurements of the true relative strain) with typical samples (thickness = 4 mm.) as shown on figure 4. The tensile tests were conducted at different temperatures (with different samples for each temperature) and consisted of loading/unloading with a progressive increase of monitored strain by steps of 0.5%. For each sample, the test was stopped when an irreversible strain is measured after unloading. The maximum reversible strain measured is plotted on figure 5 as a function of the temperature for the both alloys. One can notice that the best superelastic properties (2% of reversible strain) are obtained for a temperature just above the $R_s\#A_f$ temperature. This trend confirms that the best superelastic properties are closely related to the occurrence of R phase transformation under applied stress/strain. The best superelastic properties are obtained at temperatures ranging from 30°C up to 60°C for $\text{Ti}_{50}\text{Ni}_{50}$ (as already discussed, the binary alloy has been cold-worked and annealed) alloy, and at temperatures ranging from -25°C up to 0°C for $\text{Ti}_{50}\text{Ni}_{48}\text{Fe}_2$ alloy.

These results show that it is possible to obtain superelastic properties at temperatures below 0°C on SMA of TiNiFe type, without cold-working and the subsequent annealing at 350-500°C as it is necessary for binary TiNi alloy.

Charpy impact test were conducted for temperatures ranging from -196°C up to +50°C on samples of 55mm length, 10mm width and 2.5mm in thickness. Figure 6 summarizes the impact energy curves obtained on both alloys as a function of the test temperature. One can notice an unexpected trend, showing a high brittle behaviour at +50°C for equiatomic TiNi and at -25°C for TiNiFe alloy. Some complementary fractograph examinations have confirmed a non-ductile fracture mode (quasi-cleavage mode?) for the samples failed in this temperature range. For other temperatures, a fully ductile fracture area is observed.

It is quite surprising that these temperatures correspond to the higher superelastic response of the both alloys as observed earlier. So, these results seem to indicate that the occurrence (under stress) of "R" phase promotes a high brittleness. This is of technological importance since optimization of superelastic properties might be detrimental to ductility/toughness of TiNi-SMA.

References

- [1] Hwang C. M. et al., Phil. Mag. A., Vol. 47, No 1 (1983), 9-62.
- [2] Salamon M. B. et al., Physical Review B, Vol. 31, No 11 (June 1985), 7306-7315.
- [3] Kuentzler R., Dossmann Y., JP IV, Coll. C4, Vol. 1 (Nov. 1991), 53-57.
- [4] Lin H.C. et al., Metall. & Mat. Trans. A, Vol. 26A (April 1995), 851-858.
- [5] Filip P. et al., Mat. Sci. & Eng., A141 (1991), L5-L8.
- [6] Morawiec H. et al., JP IV, Coll. C2, Vol. 5 (Feb. 1995), 205-210.
- [7] Treppmann D., Hornborg E., JP IV, Coll. C2, Vol. 5 (Feb. 1995), 211-216.
- [8] Lin H. C., Wu S. K., Acta Metall. Mater., Vol. 42, No5 (1994), 1623-1630.
- [9] Hoshiya T. et al., JNM 179-181 (1991), 1119-1122.
- [10] Olier P., Brachet J.C., Guenin G., JP IV, Coll. C2, Vol. 5 (Feb. 1995), 217-222.
- [11] Olier P. et al., to be published in the proceeding of "ESOMAT '97", JP IV.
- [12] Escher K., Huhner M., Pract. Met. 27 (1990), 231-235.

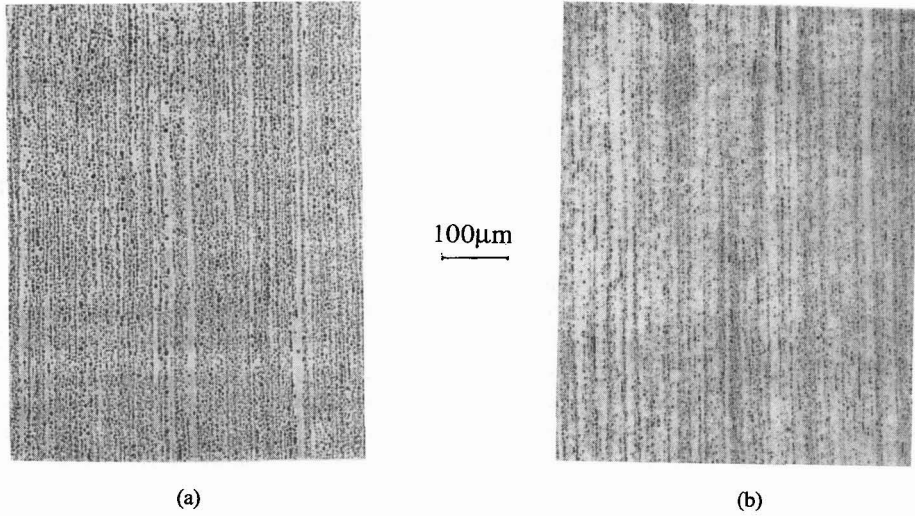


Figure 1 : Optical micrographs (after electrolytic polishing) showing the precipitation in TiNi (a) and TiNiFe (b).

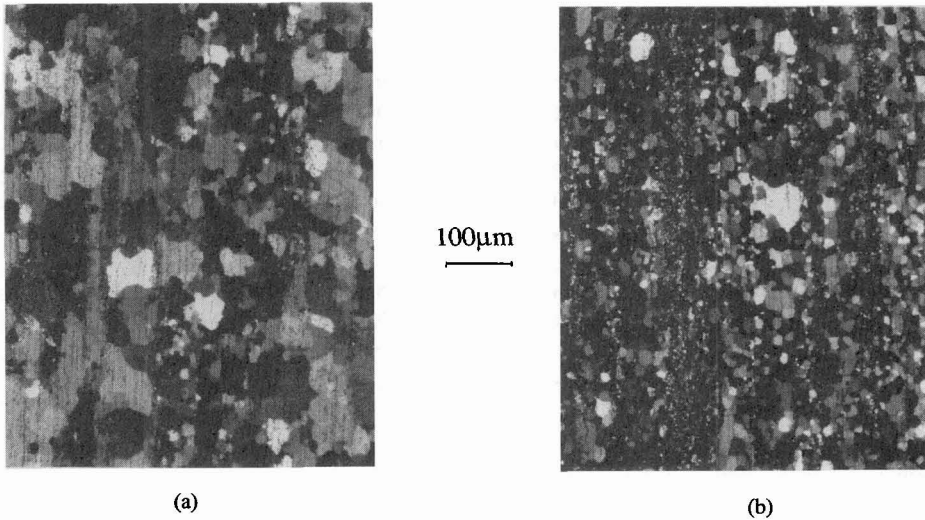


Figure 2 : Optical micrographs (after colour etching - polarized light) showing the grain size in TiNi (a) and TiNiFe (b).

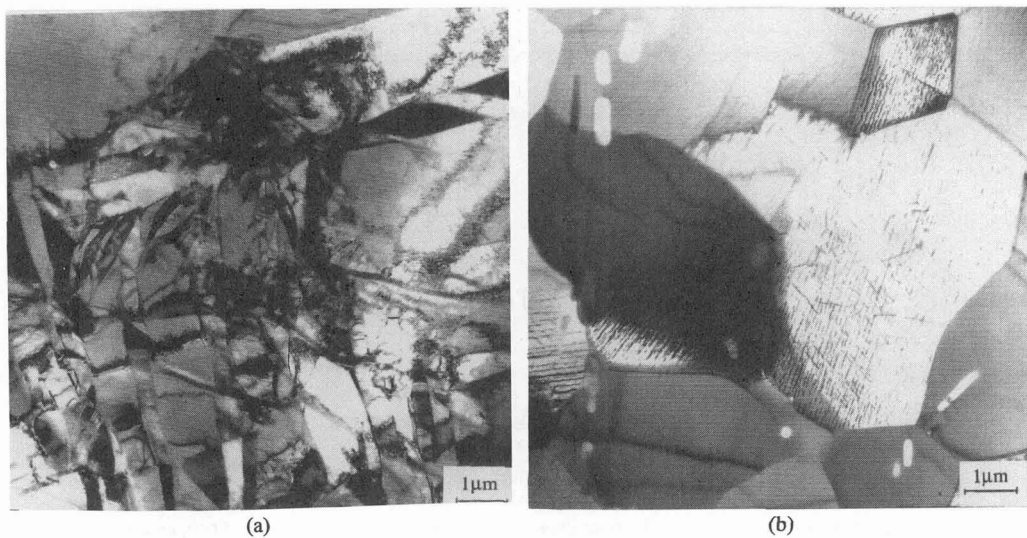


Figure 3 : TEM micrographs showing the matrix biphased structure of TiNi (a) and the austenitic structure of TiNiFe (b).

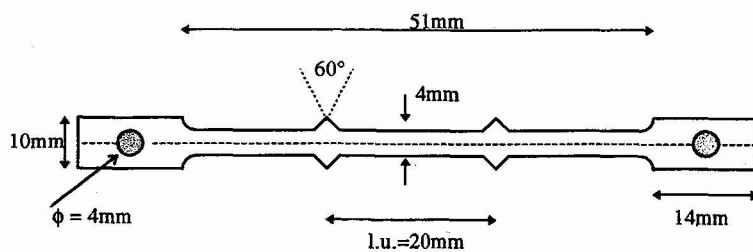


Figure 4 : Tensile samples used for superelasticity measurements as a function of temperature.

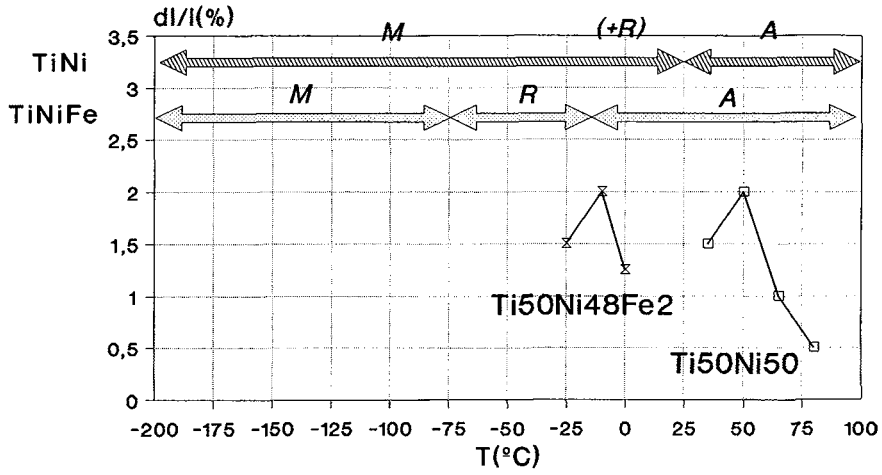


Figure 5 : Maximum reversible strain obtained from tensile test as a function of temperature.

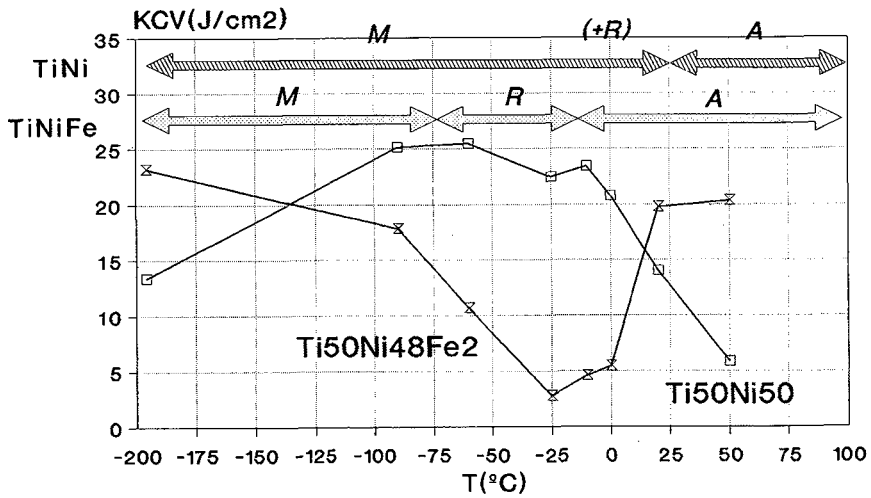


Figure 6 : Charpy impact properties as a function of test temperature.